

Supplementary information

Carbonized Silk Georgette as Ultrasensitive Wearable Strain Sensor for Full-Range Human Activity Monitoring

Chunya Wang,^{a,b} Kailun Xia^{a,b}, Muqiang Jian^{a,b}, Huimin Wang^{a,b}, Mingchao Zhang^{a,b}
and Yingying Zhang^{a,b*}

^a Key Laboratory of Organic Optoelectronics and Molecular Engineering of the Ministry of Education, Department of Chemistry, Tsinghua University, Beijing 100084, PR China.

^b Center for Nano and Micro Mechanics (CNMM), Tsinghua University, Beijing, 100084, P. R. China.

*Corresponding Author. Email: yingyingzhang@mail.tsinghua.edu.cn

This supplementary file includes:

- Supplementary Figure S1 to S11
- Supplementary Table S1

Supplementary discussions related to the equivalent circuit model for estimating the resistance change of CSG-based strain sensor with applied strain (Figure S8).

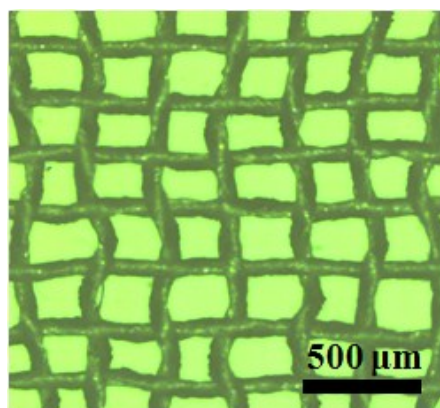


Figure S1. Optical image of a pristine silk georgette.

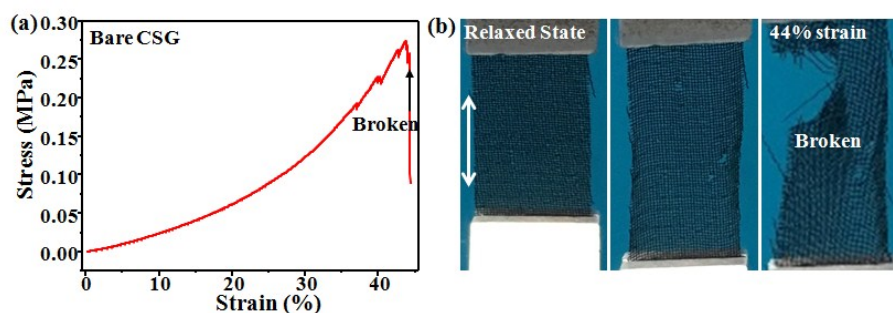


Figure S2. (a) The stress-strain curve of the bare CSG. (b) Optical photographs of the bare CSG under tensile strain.

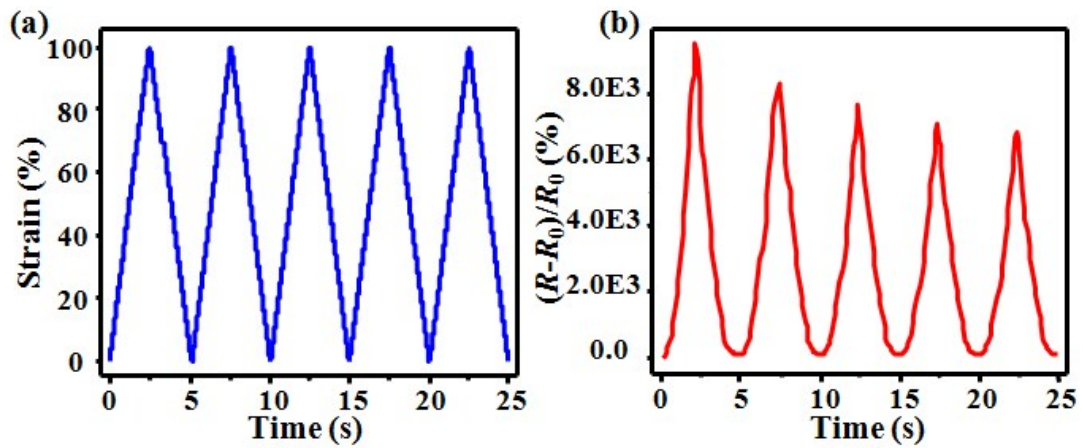


Figure S3. (a) Cyclic tensile strain loaded on the CSG-based strain sensor. (b) The corresponding relative resistance change of the sensor under cyclic strain (100%).

Noted that the overshoot of the incipient cycles, as shown in Figure S3b, can be contributed to the viscoelasticity of the PDMS. .

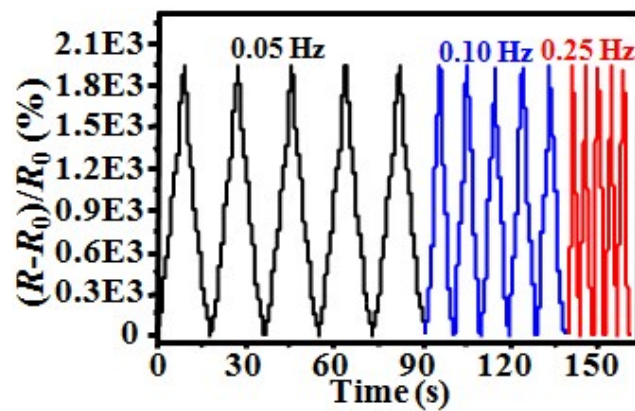


Figure S4. Relative resistance change of the CSG-based strain sensor under cyclic tensile strain (50%) with frequency of 0.05, 0.10, and 0.25 Hz.

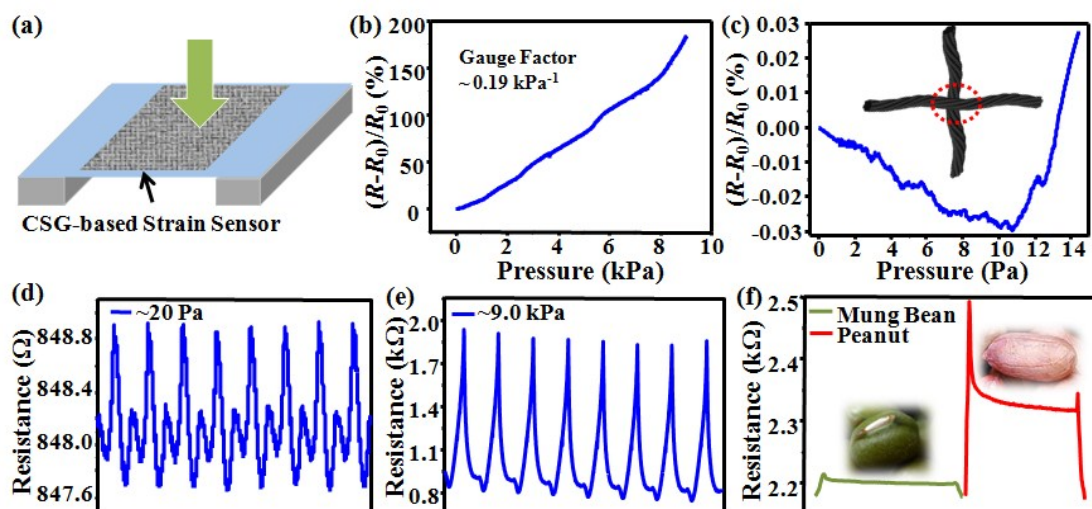


Figure S5. Sensing performance of the CSG-based pressure sensor. (a) Schematic

illustration of the CSG-based pressure sensor based on the cavity design. (b) Relative resistance change versus applied pressure, displaying a good sensitivity of $\sim 0.19 \text{ kPa}^{-1}$. (c) Close-up of Relative resistance change versus applied pressure at low pressure. (d, e) Resistance response to cyclic loading of low pressure of 20 Pa (d) and high pressure of 9.0 kPa (e). (f) Resistance response for detection of a mung bean ($\sim 69 \text{ mg}$) and a peanut ($\sim 749 \text{ mg}$).

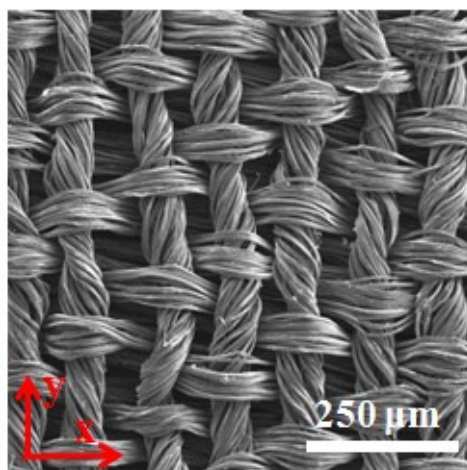


Figure S6. SEM image of the other side of carbonized satin-weave silk fabric.

Table S1. Comparison of sensing performance between strain sensors based on carbonized silk fabric with different structures.

Carbonized fabric based strain sensors	Workable strain range	Average Gauge Factor
Silk georgette	100%	29.7 (0-40%); 173.0 (60%-100%)
Plain-weave fabric	500%	9.6 (0-250%); 37.5 (250-500%)
Satin-weave fabric	280%	6.1 (0-140%); 17.2 (140-280%)
Twill-weave fabric	370%	3.5 (0-180%); 19.1 (180-370%)

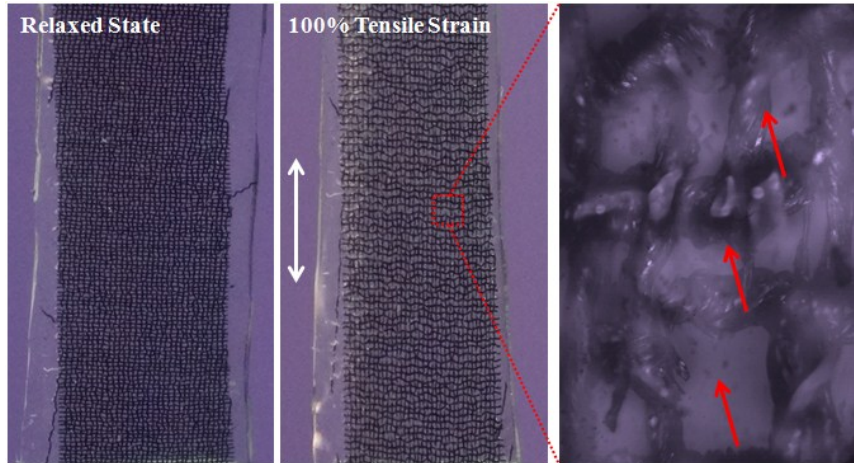


Figure S7. Optical photographs of CSG-based strain sensor in relaxed and stretched (100% tensile strain) states and corresponding optical microscopy image of the fractured structure (indicated by arrows) in stretched state.

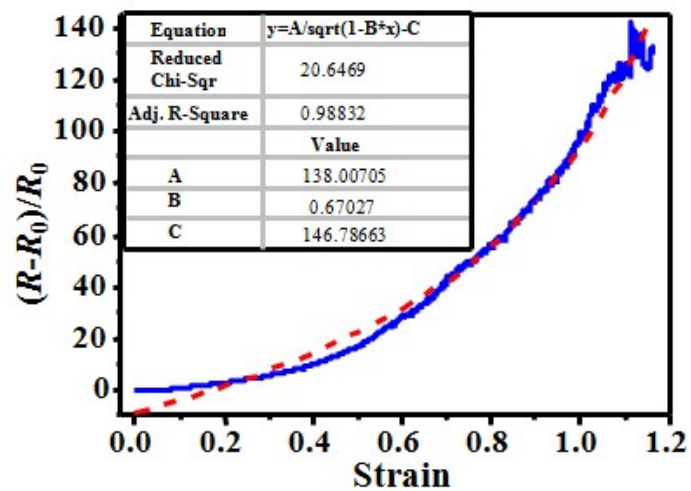


Figure S8. The fitting of this model to the experimental results.

Figure 4d illustrates the equivalent circuit model for estimating the resistance of CSG-based strain sensor, where R_1 refers to the total resistance of the intrinsic resistance of the twisted yarn in the direction perpendicular to the tensile one and the contact resistance between the yarns in the two directions, R_c refers to the contact resistance of cracked twisted yarns in the tensile direction. According to the electrical contact theory (Holm's theory)^[1], R_c could be defined as follows:

$$R_c = \frac{\rho}{2} \sqrt{\frac{H}{nP}}$$

where ρ , H , A and P refers to the electrical resistivity of carbonized twisted yarns, the

material hardness, the number of contact points and the contact pressure between fractured twisted yarns, respectively. The electrical resistivity and material hardness are constant for a given material. The number of contact points decreased with the applied strain, generating the increased contact resistance. According to the equivalent circuit model shown in Figure 4d, the resistance of the CSG-based strain sensor could be calculated as follows:

$$R = \frac{n}{m} (R_c + R_1)$$

During the tensile strain, R_1 is assumed to be constant, the number of contact points between fractured twisted yarns decreases with the strain and is defined as follows:

$$A = A_0 - k\varepsilon \quad (\varepsilon: \text{strain})$$

Accordingly, the relative resistance change of the CSG-based strain sensor could be calculated and modified with modifying coefficient of A, B, and C as follows:

$$\frac{\Delta R}{R_0} = \frac{A}{\sqrt{1 - B\varepsilon}} - C$$

The fitting of this calculated relative resistance change to the experimental results is shown in Figure S6, which showed good fitting.

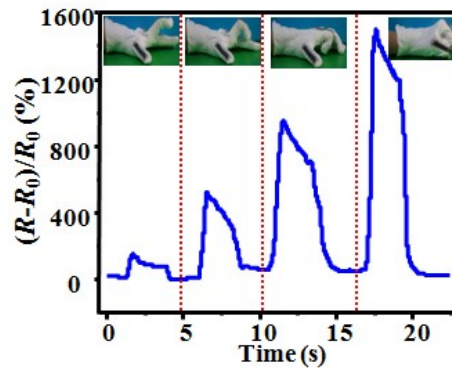


Figure S9. Relative resistance change versus time corresponding to the bending of index finger.



Figure S10. Photographs showing the CSG-based stain sensor attached on a running tights for monitoring respiration..

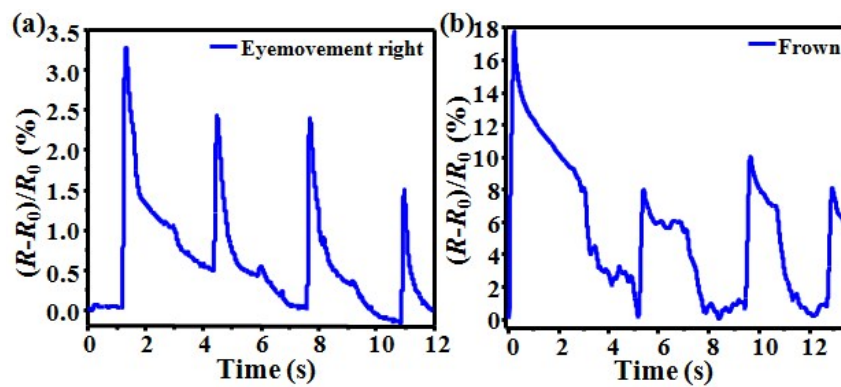


Figure S11. Relative resistance change versus time corresponding to the eyeball movement to the right (a) and frown (b).

Reference

[1] Armingto.Re, *Ieee Spectrum* **1967**, 4 10, 132.